

Quantum Diffusion Induced by Small Quantum Chaos

Hiroaki S. Yamada

Yamada Physics Research Laboratory, Aoyama 5-7-14-205, Niigata 950-2002, Japan

Kensuke S. Ikeda

College of Science and Engineering, Ritsumeikan University, Noji-higashi 1-1-1, Kusatsu 525-8577, Japan

(Dated: January 2, 2024)

It is demonstrated that quantum systems classically exhibiting strong and homogeneous chaos in a bounded region of the phase space can induce a global quantum diffusion. As an ideal model system, a small quantum chaos with finite Hilbert space dimension N weakly coupled with M additional degrees of freedom which is approximated by linear systems is proposed. By twinning the system the diffusion process in the additional modes can be numerically investigated without taking the unbounded diffusion space into account explicitly. Even though N is not very large, diffusion occurs in the additional modes as the coupling strength increases if $M \geq 3$. If N is large enough, a definite quantum transition to diffusion takes place through a critical sub-diffusion characterized by an anomalous diffusion exponent.

PACS numbers: 05.45.Mt, 73.43.Cd, 05.00.00, 05.60.Gg

Introduction.- By introducing any perturbation to completely integrable systems, chaotic region is formed close to the nonlinear resonance which exists almost everywhere in the phase space. However, chaotic components are prevented to globalize by the KAM tori and are localized [1, 2]. However, if such a small localized chaos interacts with some additional degrees of freedom, it can drive them and can change their energies on a large scale.

A typical example is the mechanism proposed by Arnold [3]. He showed that the entanglement between the stable and unstable manifolds of the unstable fixed point of a resonance, which causes the so called stochastic layer chaos, simultaneously leads to the intersection of stable and unstable manifolds with different energies of the additional degrees of freedom, thereby forming a global path to change their energy. Such kind of global instability is called the Arnold diffusion and were treated analytically and numerically [2, 4–7]. The global motion induced by a localized small chaos such as the stochastic layer is an initiation leading to the intrinsically global ergodic motions [2, 8–10].

Investigations of quantum Arnold diffusion for various systems elucidated that quantum motion mimics the classical delocalization. [11–14]. However, the diffusion rate is much smaller than the classical one and very long-time behavior of the quantum diffusion is not known. It is expected to be suppressed by the quantum localization effect [13–15].

So far the quantum chaotic diffusion has been investigated extensively for “large” quantum chaos system defined in unbounded phase space with infinite Hilbert-space dimension [16–19]. In such systems chaotic degrees of freedom itself may actively exhibit diffusion in the classical limit, but the diffusion is inhibited in its quantum counterparts due to the quantum localization effect. Such quantum localization is, however, destroyed, and classical diffusion is recovered [20, 21] through Anderson-like transition if the number of degrees of freedom increases

[18, 19, 22–24]. On the other hand, the nature of quantum diffusion *passively induced by small quantum chaos system* have not been known, although it is a fundamental problem closely related to the quantum global instability such as the Arnold diffusion.

In the present paper, we propose a simple model and method, with which we can examine whether or not a small quantum chaos can induce global diffusive motion along the modes contacting with it, and show that a global transportation is realized under appropriate conditions. “Small chaos” means chaotic systems confined to a finite region of the phase space by geometrical or dynamical conditions in the classical limit. As a first step, we examine small but sufficiently unstable chaos. Small and weakly unstable chaos such as stochastic layer will be investigated in forthcoming papers.

Model.- As the first class of example, we consider strong and uniform chaotic systems called as C-system or K-system bounded finitely by periodic boundaries [1], which are coupled with several number of unbounded additional degrees of freedom. The former is referred to as the main system and latter as the additional modes, respectively. The additional modes are supposed to be integrable if isolated, as is the example considered by Arnold. They are coupled weakly with the former at a small coupling strength characterized by the parameter η .

We suppose the integrable additional modes of number M is initially located at the action eigenstate $|I_{0k}\rangle$ ($1 \leq k \leq M$) where $I_{0k} = \hbar \times \text{integer}$. We approximate the Hamiltonian of the additional modes by linearizing around $I_k \sim I_{0k}$, and reset $\hat{I}_k - I_{0k}$ by \hat{J}_k . Then Hamiltonian of the entire system is represented by

$$\begin{aligned} \hat{H}(\hat{p}, \hat{q}, \hat{J}, \hat{\phi}, t) &= \hat{\mathcal{H}}(\hat{p}, \hat{q}, \hat{\phi}, t) + \hat{h}(\hat{J}) \\ \hat{\mathcal{H}}(\hat{p}, \hat{q}, \hat{\phi}, t) &= \hat{p}^2/2 + V(\hat{q})\Delta(t) + \eta v(\hat{q})w(\hat{\phi})\Delta(t), \end{aligned} \quad (1)$$

where $\Delta(t) := \sum_{n \in \mathbb{Z}} \delta(t - n)$ is the periodic delta-

functional kicks. $\hat{h}(\hat{\mathbf{J}}) = \boldsymbol{\omega}\hat{\mathbf{J}}$, where $\hat{\mathbf{J}} = (\hat{J}_1, \dots, \hat{J}_M)$, and $\boldsymbol{\omega} = (\omega_1, \dots, \omega_M)$ are the linear frequencies at $I_k = I_{0k} (k = 1, \dots, M)$. They are supposed to be mutually incommensurate. $\hat{\boldsymbol{\phi}} = (\hat{\phi}_1, \dots, \hat{\phi}_M)$ are the angle operators conjugate to action operators \hat{J}_k as $\hat{J}_k = -i\hbar\partial/\partial\phi_k$ in the c-number representation of $\hat{\phi}_k$ ($0 \leq \phi_k \leq 2\pi$). We take $w(\hat{\boldsymbol{\phi}}) := \sum_{k=1}^M w(\hat{\phi}_k)$, where $w(\phi_k)$ is a 2π periodic function of angle variable ϕ_k with mean value 0.

Here, we take the main system represented by as a kicked rotor driven by the periodic kick $\Delta(t)$ of period 1 applied to the potential $V(\hat{q})$, where $\hat{q} = \sum_q q|q\rangle\langle q|$ and $\hat{p} = \sum_p p|p\rangle\langle p|$ are the position and momentum operators with eigenvalues q and p , respectively.

The main system is confined in the bounded phase space $-\pi \leq p \leq \pi$, $-\pi \leq q \leq \pi$, and the periodic boundary conditions are imposed on p and q . Then they are quantized as $q = \ell\hbar$ and $p = \ell'\hbar$, where ℓ, ℓ' are the integers satisfying $-N/2 \leq \ell, \ell' \leq N/2$ with N being the Hilbert-space dimension of the main system related to the Planck constant as $\hbar = 2\pi/N$.

Next, we take the Arnold cat map $V(\hat{q}) = K\hat{q}^2/2$ or the standard map $V(\hat{q}) = K\cos\hat{q}$ defined in the above bounded phase space as the main system $H_0(\hat{p}, \hat{q}, t)$. Taking $K(\in \mathbb{Z})$ as $K > 4$ or $K < 0$ (cat map) or $|K| \gg 1$ (standard map) the main system can be made C-system and approximately K-system, respectively, which are (almost) uniformly chaotic with a flat invariant measure in the classical limit. The interaction terms $v(q)$ and $w(\phi)$ are period 2π -functions of q and ϕ , respectively, with 0 mean for the uniform invariant measure. We choose $v(q) = \cos(q)$ and $w(\phi_k) = \cos\phi_k$ of the interaction term in this paper. The similar model with linear oscillators have been used by several authors while studying the chaotic dynamics of the rotors [25] and Anderson transition of the atomic matter waves [26, 27].

A great merit of using the linear oscillators as the additional mode is that the unitary evolution operator $\hat{U}(t) = \mathcal{T}\exp\{-i\int_0^t \hat{H}(\hat{p}, \hat{q}, \hat{J}, \hat{\boldsymbol{\phi}}, s)ds/\hbar\}$ can be factorized into the action-dependent part and angle-dependent part as

$$\begin{aligned} \hat{U}(t) &= e^{-i\hat{h}(\hat{\mathbf{J}})t/\hbar}\hat{U}(t, \hat{\boldsymbol{\phi}}), \\ \hat{U}(t, \hat{\boldsymbol{\phi}}) &:= \mathcal{T}e^{-\frac{i}{\hbar}\int_0^t \hat{\mathcal{H}}(\hat{p}, \hat{q}, \hat{\boldsymbol{\phi}} + \boldsymbol{\omega}s)ds}, \end{aligned} \quad (2)$$

where \mathcal{T} means the time-ordering operator. If the operator \hat{X} does not contain the angle operators, the time evolved operator $\hat{X}(t) = \hat{U}^\dagger \hat{X} \hat{U}$ is dominated by $\hat{U}(t)$ as $\hat{X}(t) = \hat{U}(t)\hat{X}\hat{U}(t)$. The action $\hat{J}(t)$ changes only at the $t = n(n \in \mathbb{Z})$ -th kick. The Heisenberg equation of motion $d\hat{J}/dt = i[\hat{\mathcal{H}}, \hat{J}]/\hbar$ is integrated at each kick to leads to

$$\hat{J}_k(t) - \hat{J}_k(0) = -\sum_{n=1}^{[t]} \eta v(\hat{q}(n))w'(\hat{\phi}_k + \omega_k n), \quad (3)$$

where $[]$ is the Gauss symbol and $w'(\phi_k) := dw(\phi_k)/d\phi_k$. Our interest is whether or not the chaotic motion of

the main system can induce a global transport in the action space starting from $|\mathbf{J} = 0\rangle$. The physical quantity directly measuring the transported distance is the mean square displacement (MSD) of the action: $\Delta J_k(t)^2 := \langle \Psi_0 | (\hat{J}_k(t) - \hat{J}_k(0))^2 | \Psi_0 \rangle$ ($k = 1, 2, \dots, M$), where $|\Psi_0\rangle = |\psi_0\rangle_{|\mathbf{J}=0}$ and $|\psi_0\rangle$ is the initial state of the main system. Classically, Eq.(3) describes a typical situation in which chaos induces diffusion in the additional modes: if the main system is fully chaotic, the 'force' $v(q(n))w'(\phi_k + \omega_k n)$ is completely random with 0 mean, and the classical variable $\Delta J_k(t)$ exhibits a Brownian motion. To compute the MSD or higher-order moment, we need not explicitly taking the infinite Hilbert dimension of the J -space into account as shown below.

Method.- We twin the two identical parts represented by the Hamiltonian $\hat{\mathcal{H}}(\hat{p}, \hat{q}, \hat{\boldsymbol{\phi}}, t)$ of Eq.(1) and its paired one $\hat{\mathcal{H}}(\hat{p}', \hat{q}', \hat{\boldsymbol{\phi}}, t)$. Returning t to the continuous time representation, the Hamiltonian \hat{H}_T of the twinned system is

$$\begin{aligned} \hat{H}_\xi^T &= \hat{\mathcal{H}}_\xi^T(\hat{p}, \hat{q}, \hat{\boldsymbol{\phi}}, t) + h(\hat{\mathbf{J}}) \\ \hat{\mathcal{H}}_\xi^T &:= \hat{\mathcal{H}}(\hat{p}, \hat{q}, \hat{\boldsymbol{\phi}}, t) + \hat{\mathcal{H}}(\hat{p}', \hat{q}', \hat{\boldsymbol{\phi}}, t) + \xi\hat{W}(\hat{\phi}_k, t). \end{aligned} \quad (4)$$

The second part is spanned by the coordinate basis $|q'\rangle$ or the momentum basis $|p'\rangle$, and $\hat{q}' := \sum_q q|q'\rangle\langle q'|$ and $\hat{p}' := \sum_p p|p'\rangle\langle p'|$ are its coordinate and momentum operators, respectively. \hat{W} is the interaction between the twinned parts given by

$$\hat{W}(\hat{\phi}_k, t) := w'(\hat{\phi}_k) \sum_q v(q)(|q\rangle\langle q'| + |q'\rangle\langle q|)\Delta(t-0), \quad (5)$$

The twin system is illustrated in Fig.1(a). The interaction between the twins takes place just at $t = n+0 (n \in \mathbb{Z})$ after the periodic kick. We define here the transition operators $\hat{R}^+ = \sum_q |q'\rangle\langle q|$ and $\hat{R}^- = (\hat{R}^+)^\dagger$. Since our the system is formed by twins and the non-interacting Hamiltonian $\hat{H}_{\xi=0}^T$ commutes with \hat{R}^\pm , the time-evolved operators \hat{R}^\pm change only in the moments of the interaction at $t = n+0$. Let $\hat{U}_\xi^T(t)$ and $\hat{U}_\xi^T(t)$ be the time evolution operator of the Hamiltonian \hat{H}_ξ^T and $\hat{\mathcal{H}}_\xi^T(\hat{p}, \hat{q}, \hat{\boldsymbol{\phi}} + \boldsymbol{\omega}t)$, respectively. Then the relation similar to Eq.(2) holds and $\hat{R}^\pm(t)$ is dominated by $\hat{\mathcal{H}}_\xi^T(\hat{p}, \hat{q}, \hat{\boldsymbol{\phi}} + \boldsymbol{\omega}t)$. As a result, we obtain

$$\begin{aligned} &(\hat{R}^+(t) - \hat{R}^+(0))/\xi \\ &= \frac{i}{\hbar} \sum_{s=1}^{[t]} [v(\hat{q}(s)) - v(\hat{q}'(s))]w'(\hat{\phi}_k + \omega_k s). \end{aligned} \quad (6)$$

We suppose initially the second chaotic system is not populated, and only the first main system and the additional modes are started from the same initial condition as the original system given by Eq.(1). Here the coupling strength ξ of the twinned system is chosen at the

smallest level within the numerical precision allows. The RHS of Eq.(6) is computed in the lowest order with respect to ξ . Then the second term of RHS, which contains only the population operator of the second system, can be neglected, and the LHS of Eq.(6) is identified with $\hat{J}_k(t) - \hat{J}_k(0)$. The MSD is thus related to the excitation number $\hat{R}^+ \hat{R}^-$ as

$$\begin{aligned} \Delta J_k(t)^2 &:= \langle \Psi_0 | (\hat{J}_k(t) - \hat{J}_k(0))^2 | \Psi_0 \rangle \\ &= \langle \Psi_0 | (\hat{R}^+(t+0) - \hat{R}^+(0)) (\hat{R}^-(t+0) - \hat{R}^-(0)) | \Psi_0 \rangle / \xi^2 \\ &\simeq \frac{\hbar^2 \eta^2}{(2\pi)^M \xi^2} \int d\phi \sum_q |\langle q | \hat{U}_\xi^T(t, \phi) | \psi_0 \rangle|^2, \end{aligned} \quad (7)$$

where $\int d\phi = \int_0^{2\pi} \dots \int_0^{2\pi} \prod_k^M d\phi_k$. As mentioned above, $\hat{U}_\xi^T(t, \phi) = \mathcal{T} \exp\{-i \int_0^t \hat{\mathcal{H}}_\xi^T(\hat{p}, \hat{q}, \phi + \omega s, s) ds / \hbar\}$, which can be expressed as the product of step-by-step evolution operator. More detailed derivation and remarks about Eqs.(6) and (7) can be found in the Appendix A. In the following we omit k from \hat{J}_k and J_k if not necessary.

Thus the MSD is copied to the total excitation number of the second main system. The higher-order moment can also be evaluated in the same way. The integration over the phase variables ϕ means to take quantum mechanical average with respect to the initial action state $|\mathbf{J} = \mathbf{0}\rangle = \int_0^{2\pi} \dots \int_0^{2\pi} d\phi |\phi\rangle / (2\pi)^{M/2}$ which is very efficiently carried out by replacing the integral by the average over quasi random numbers of the integer(ν)-multiplied irrational number $\phi_k = \nu \chi_k$ ($0 \leq \nu \leq \nu_{max}$), where χ_k are irrational numbers.

We have only to execute the numerical wavepacket evolution with $\hat{U}_\xi^T(t, \phi)$ using $2N$ -dimensional basis for fixed c-number $\phi_k = \nu \chi_k$ starting from $|\psi_0\rangle$, and compute the integrand of Eq.(7) for a fixed $\phi_k = \nu \chi_k$, and next take the average over the ν_{max} data. Finally the average over the results for randomly chosen initial state $|\psi_0\rangle$ is taken.

We compared the result of the twinning method with the result of the direct wavepacket propagation in the full Hilbert space spanned by the truncated set of action basis and the N -dimensional basis of main system. The results agree well, which are demonstrated in the Appendix A.

Result. - We first take the chaotic cat map as the main system, which induces ideal Diffusion process according to Eq.(3) in the classical model. However in the quantum version follows the classical chaotic diffusion at least in a certain period of time evolution. Indeed, in the case of $M = 1$, the diffusion is suppressed and the MSD reaches to an upper bound $\ell^2 := \Delta J^2(t = \infty)$ (for brevity the index k is omitted). We call ℓ the quantum localization length. Numerically $\ell \propto N^2 D_{cl}$, where D_{cl} is classical diffusion constant proportional to η^2 , which is predicted by a simple theoretical consideration. (See Appendix B.) For $M = 2$, the classical diffusion is still suppressed, but the numerical observation tells that localization length is enhanced and increases exponentially as $\ell \propto \exp\{D_{cl} N^2\}$ [28, 29]. (See Appendix B.)

As $M \geq 3$, things changes drastically: for small enough η the MSD still saturates at a finite level and the quan-

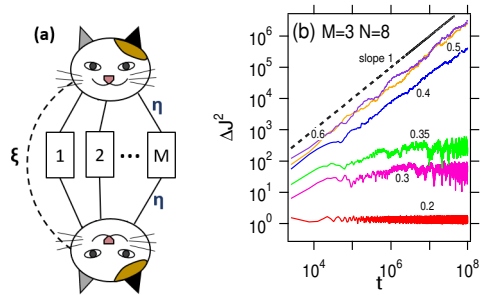


FIG. 1: (Color online) (a) An Illustration of the twinned system with the coupling strength η and ξ . (b) The double-logarithmic plots of $\Delta J^2(t)$ as a function of time for the perturbed cat map for $K = -1$ of $N = 8$ with trichromatic perturbation ($M = 3$). The result for various η in the range $\eta \in [0.2, 0.6]$ is shown.

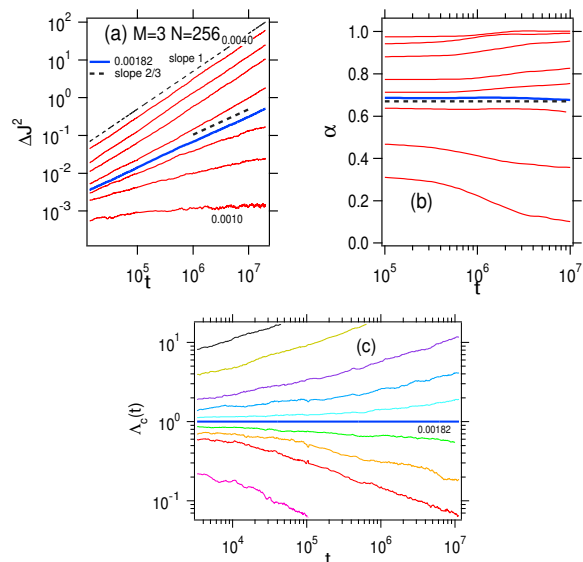


FIG. 2: (Color online) (a) The double-logarithmic plots of $\Delta J^2(t)$ as a function of time for the perturbed cat map for $K = -1$ of $N = 256$ with trichromatic perturbation ($M = 3$). The results for $\eta_c \simeq 0.00182$ is shown in thick blue line. The broken lines with the slope 1 and 2/3 are shown. (b) The instantaneous diffusion index $\alpha(t)$ for some ϵ . The broken line indicates the critical subdiffusion line $\alpha(t) = \alpha_c = 2/3$ predicted by the scaling theory. (c) The scaled MSD $\Lambda_c(t)$ as functions of time for increasing perturbation strengths. The range is $\eta \in [0.001, 0.004]$.

tum localization still remains, but as η is taken large enough the MSD increases linearly without limit at least for t less than 10^8 . Figure 1(b) shows that such a drastic change is observed even for very small main system with N of only 8. The border between the localization and the normal diffusion is not, however, very definite. (See Appendix C.) On the other hand, as N increases greater than 10^2 the transition from localization to the normal diffusion becomes very definite. Figure 2 presents a typical example of $N = 256$. There exists a critical

value $\eta = \eta_c$ below which the MSD saturates and above which the MSD increases to reach to the normal diffusion. And just at $\eta = \eta_c$ the MSD increases according to an anomalous diffusion law $\Delta J^2(t) \propto t^\alpha$ with a characteristic exponent α ($0 \leq \alpha \leq 1$). Figure 2(b) shows the temporal behavior of MSD around $\eta = \eta_c$ by using the time-dependent characteristic exponent $\alpha(t)$ defined by

$$\alpha(t) = \frac{d \log \overline{\Delta J^2(t)}}{d \log(t)}, \quad (8)$$

where the over-line $\overline{X(t)}$ means to take a local time average of $X(t)$. Eq.(8) implies $\overline{\Delta J^2(t)}$ increases $t^{\alpha(t)}$ locally at t .

Figure 2(b) shows the $(t, \alpha(t))$ -plot for various η . Below η_c , $\alpha(t)$ decreases monotonically to zero, while it increases to reach the normal diffusion $\alpha = 1$ above η_c , which provides a strong evidence that a definite transition from the localization to the normal diffusion without limit takes place. Just at $\eta = \eta_c$, $\alpha(t)$ takes a constant value α_c and MSD exhibits an anomalous diffusion $\Delta J^2_{\eta=\eta_c}(t) \propto t^{\alpha_c}$. As η exceeds η_c , the diffusion constant approaches to the classical diffusion constant $D_{cl} \propto \eta^2$.

Once η_c is decided by the $(t, \alpha(t))$ -plot, the critical behavior close to η_c can be more directly captured by the scaled representation of MSD $\Lambda_c(t) := \Delta J^2(t) / \Delta J^2_{\eta=\eta_c}(t)$ as shown in Fig.2(c). The critical value η_c decreases very rapidly with N , which will be discussed later.

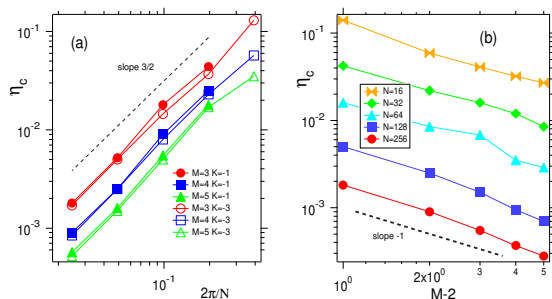


FIG. 3: (Color online) (a) The critical perturbation strength η_c as a function of $h = 2\pi/N$ for the perturbed cat map with $M = 3, 4, 5$ and $K = -1, -3$. The black broken line with a slope 3/2 is shown. (b) η_c as a function of $M - 2$ for $K = -1$. The black dotted line with a slope -1 is shown. Note that the data are plotted in double-logarithmic scale.

The localization-diffusion transition is always observed if $M \geq 3$ and the MSD increases according to the subdiffusion $\Delta J^2(t) \propto t^{\alpha_c}$ at the critical η_c , which decreases as $\eta_c \sim N^{-3/2}$, as shown in Fig.3(a), if $N \gg 1$. According to the numerical observation α_c is independent of N and depends only on M and decreases to zero with M . The critical value η_c also decreases with M as shown in Fig.3(b). The results are summarized as

$$\alpha_c = \frac{2}{M}, \quad \eta_c \propto N^{-3/2}(M-2)^{-1}. \quad (9)$$

The diffusion phenomena can never be observed for the elliptic cat ($-4 < K < 1$), if $N \gg 1$ and η is small enough. The results mentioned above does not change if the main system is replaced by the standard map of $|K| \gg 1$ defined on a periodically bounded phase space.

The transition scheme through the critical subdiffusion $\Delta J^2(t) \sim t^{2/M}$ is very similar to the Anderson-like transition observed for standard map perturbed by multiply-periodic perturbations [22–24]. It is, however, basically different from ours in that the diffusive motion is supported by the chaotic degree of freedom itself. It is a large quantum chaotic system defined in an infinitely extended phase space and is supported by infinite dimensional Hilbert space.

An alternative model.— Next, we examine a more natural case where a non-ideal chaos generated by the overlap of two nonlinear resonances is bounded finitely not by the periodic boundaries but by regular orbits. We take a modified standard map defined as follows. The potential is $V(\hat{q}) = K \cos \hat{q}$ as usual, and the momentum space is unbounded. But the kinetic energy takes the ordinary form $T(\hat{p}) = \hat{p}^2/2$ only in a bounded region $I := [p_1, p_2]$, and $T(\hat{p})$ is replaced by linear functions $a\hat{p} + b$ out of I . The constants a and b are decided such that $T(\hat{p})$ is continuous and smooth at p_1 and p_2 . It is easy to show the classical motion outside of I is completely integrable. By choosing p_1 and p_2 adequately, we can confine the two resonances at $p = 0$ and $p = 2\pi$, which yields chaotic motion by the overlap of resonances for $K > 1$, as is illustrated in Fig.4(a). Thus our system models typical situation of a small classical chaos bounded by regular regions.

We examined the above system by our method. The obtained results is not so simple as the ideal case of the cat map, but we confirmed that the normal diffusion is recovered for $M \geq 3$ following a similar scenario as the cat map. We show in Fig.4(b) the transition process of MSD together with the classical Poincare plot of the main system.

Conclusion.— In conclusion we investigated whether small quantum chaos can induce quantum diffusion leading to the global transportation. As a simplest model we proposed a small but strong quantum chaos system coupled very weakly with additional linear modes. The existence of diffusion depends seriously on the number M , and for $M \geq 3$ global diffusion is induced even for small Hilbert space dimension N . If $N \gg 1$ the diffusion is realized through a critical state exhibiting an anomalous diffusion as the coupling strength exceeds a weak quantum critical value. In the present work we examined sufficiently unstable chaotic systems in the classical limit as the main system. More interesting is the case of small and weakly unstable chaos typically exemplified by the stochastic layer. In the latter case the global transportation process along the linear modes corresponds to a quantum Arnold diffusion, and its existence is a quite interesting problem.

We finally note that our system may be implemented

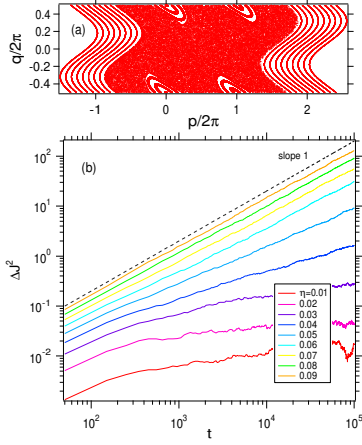


FIG. 4: (Color online) (a) The classical Poincaré map of the modified standard map, which manifests overlapped chaos around two resonances at $p = 0$ and $p = 2\pi$ is finitely bounded by tori. Here $K = 3.0$ and $M = 3$, and $p_{1,2} = \pi \pm 2\pi$. (b) Double logarithmic plots of MSD vs t for (a) are shown. Diffusion in the additional modes is recovered with increase in η , where $N = 256$ ($\hbar = 2\pi/N$).

as molecular vibration or rotation resonantly excited by a pulsed laser light. If a few number of additional weak cw laser light with different frequencies are applied as seeds, scattering of "quantum chaotic" light to the applied frequency modes are induced as a quantum phase transition. It is a novel kind of light scattering phenomenon.

Appendix A: The twinning method

1. Details of the derivation of Eqs.(4)-(7)

As presented in Eq.(2) in the main text, we decouple the action($\hat{\mathbf{J}}$)-dependent part from the unitary evolution operator of the Hamiltonian (1) in the main text. Indeed, if we suppose the decoupled form $\hat{U} = e^{-i\hat{h}(\hat{\mathbf{J}})t/\hbar}\hat{U}$, Schrödinger equation becomes

$$\begin{aligned} \frac{d\hat{U}(t, \hat{\phi})}{dt} &= -\frac{i}{\hbar}e^{-i\hat{h}(\hat{\mathbf{J}})t/\hbar}\hat{\mathcal{H}}(\hat{p}, \hat{q}, \hat{\phi}, t)e^{-i\hat{h}(\hat{\mathbf{J}})t/\hbar}\hat{U}(t, \hat{\phi}) \\ &= \hat{\mathcal{H}}(\hat{p}, \hat{q}, \hat{\phi} + \omega t, t)\hat{U}(t, \hat{\phi}) \end{aligned}$$

and $\hat{U}(t, \hat{\phi})$ takes the form of Eq.(2) in the main text. The equation of motion of the action operator $\hat{J}_k(t) = \hat{U}^\dagger \hat{J}_k \hat{U} = \hat{U}^\dagger \hat{J}_k \hat{U}$ is given by

$$\begin{aligned} \frac{d\hat{J}_k(t)}{dt} &= \frac{i}{\hbar}[\hat{\mathcal{H}}(\hat{p}, \hat{q}, \hat{\phi} + \omega t, t), \hat{J}_k(t)] \\ &= -\eta w(\hat{\phi}_k + \omega_k t)v(\hat{q}(t))\Delta(t). \end{aligned}$$

Thus \hat{J}_k changes at $t = n$ ($n \in \mathbb{Z}$) when the kick force is applied, where $\hat{q}(t)$ does not change during the kick

interaction. The change of $J_k(t)$ at $t = n + 0$ is easily evaluated, and summing all the changes up to $[t]$, Eq.(4) in the main text follows.

Next we consider the dynamics of the twins. We decompose the action dependent part from the unitary evolution operator in the same manner as follows:

$$\begin{aligned} \hat{U}_\xi^T(t) &:= \exp\left\{-\frac{i}{\hbar}\int_0^t \hat{\mathcal{H}}_\xi^T(s)ds\right\} \\ &= e^{-i\hat{h}(\hat{\mathbf{J}})t/\hbar}\hat{U}_\xi^T(\hat{\phi}, t), \end{aligned}$$

where

$$\hat{U}_\xi^T(\hat{\phi}, t) = \exp\left\{-\frac{i}{\hbar}\int_0^t \hat{\mathcal{H}}_\xi^T(\hat{p}, \hat{q}, \phi + \omega s, s)ds\right\}.$$

The transition operators \hat{R}^\pm , which evolves as

$$\begin{aligned} \hat{R}^\pm(t) &= [\hat{U}_\xi^T(t)]^\dagger \hat{R}^\pm \hat{U}_\xi^T(t) \\ &= [\hat{U}_\xi^T(\hat{\phi}, t)]^\dagger \hat{R}^\pm \hat{U}_\xi^T(\hat{\phi}, t), \end{aligned}$$

commutes with the non-interacting part of the twin Hamiltonian $\hat{\mathcal{H}}_{\xi=0}^T$, because it is formed of twins and is expanded as

$$\hat{\mathcal{H}}_{\xi=0}^T = \sum_{q_1, q_2} \hat{A}(\hat{\phi}, q_1, q_2)[|q_1\rangle\langle q_2| + |q_1'\rangle\langle q_2'|].$$

Thus $\hat{R}^\pm(t)$ changes by the inter-twin interaction \hat{W} , and the equation of motion leads to

$$\begin{aligned} \frac{d\hat{R}^\pm(t)}{dt} &= \xi \frac{i}{\hbar}[\hat{\mathcal{H}}_\xi^T(\hat{p}(t), \hat{q}(t), \hat{\phi} + \omega t), \hat{R}^\pm(t)] \\ &= \xi \frac{i}{\hbar}w'(\hat{\phi}_k + \omega_k t)(v(\hat{q}(t)) - v(\hat{q}'(t))\Delta(t - 0)). \end{aligned}$$

The time-dependent operator $\hat{X}(t)$ is evolved in time by the action-free Hamiltonian $\hat{\mathcal{H}}_\xi^T(t)$ as $\hat{X}(t) = [\hat{U}_\xi^T(t)]^\dagger \hat{X} \hat{U}_\xi^T(t)$, which contain only the angle $\hat{\phi}$ operators with regard to the harmonic degrees of freedom. Since the parameter ξ is taken very small, the change of $\hat{R}(t)$ during the interaction process is of $O(\xi)$, and the changes of $\hat{q}(t)$ and $\hat{q}'(t)$ in the RHS, which contributes $O(\xi^2)$ correction, can be neglected. Therefore,

$$\begin{aligned} \hat{R}^+(n+1) - \hat{R}^+(n) &= \xi \frac{i}{\hbar}w'(\hat{\phi}_k + \omega_k t)(v(\hat{q}(n)) - v(\hat{q}'(n))), \end{aligned}$$

which yields Eq.(6) in the main text. In accordance with the approximation, we should neglect the coupling of $O(\xi)$ in the time evolution of $\hat{q}(n)$ and $\hat{q}'(n)$ in the LHS of the above equation or the Eq.(6) in the text. Then each system evolves with each Hamiltonian $\hat{\mathcal{H}}(\hat{p}, \hat{q}, \phi, t)$ and $\hat{\mathcal{H}}(\hat{q}', \hat{p}', \phi, t)$ respectively. Further the second system is unpopulated at $t = 0$. Under such condition $v(\hat{q}')$ can be

neglected and the correspondence, which is represented correctly as

$$\frac{([\hat{\mathcal{U}}(\hat{\phi}, t)]^\dagger \hat{J} \hat{\mathcal{U}}(\hat{\phi}, t) - \hat{J})}{\eta} = -\frac{i\hbar([\hat{\mathcal{U}}_\xi^T(\hat{\phi}, t)]^\dagger \hat{R}^+ \hat{\mathcal{U}}_\xi^T(\hat{\phi}, t) - \hat{R}^+)}{\xi},$$

holds between Eq.(3) and Eq.(6) in the main text. In the above equation the LHS is evolved by the first part of

the twins alone, but in the RHS the the time evolution is due to the weakly coupling twins. This correspondence can be applied to compute arbitrary order moment of $\hat{J}_k(t) - \hat{J}_k(0)$.

The initial state is taken as $|\Psi_0\rangle = |\mathbf{J} = 0\rangle|\psi_0\rangle$, and the state of the cat $|\psi_0\rangle$ contains only the first part, and $\hat{R}^-|\psi_0\rangle = \langle\psi_0|\hat{R}^+ = 0$. Then

$$\frac{\langle\Psi_0|(\hat{J}(t) - \hat{J})^2|\Psi_0\rangle}{\eta^2} = \frac{\hbar^2\langle\Psi_0|([\hat{\mathcal{U}}_\xi^T(t)]^\dagger \hat{R}^- \hat{\mathcal{U}}_\xi^T(t) - \hat{R}^-)([\hat{\mathcal{U}}_\xi^T(t)]^\dagger \hat{R}^+ \hat{\mathcal{U}}_\xi^T(t) - \hat{R}^+)|\Psi_0\rangle}{\xi^2}.$$

Further the angle-representation of the action eigenstate is

$$|\mathbf{J} = 0\rangle = \int_0^{2\pi} \dots \int_0^{2\pi} |\phi\rangle d\phi / (2\pi)^{M/2},$$

where $d\phi = \prod_i^M d\phi_i$. We thus have

$$\frac{\langle\Psi_0|(\hat{J}(t) - \hat{J})^2|\Psi_0\rangle}{\eta^2} = \frac{\hbar^2}{\xi^2(2\pi)^M} \int_0^{2\pi} \dots \int_0^{2\pi} d\phi \langle\psi_0|\langle\phi|([\hat{\mathcal{U}}^T(\hat{\phi}, t)]^\dagger \hat{R}^- \hat{R}^+ \hat{\mathcal{U}}^T(\hat{\phi}, t)|\phi)|\psi_0\rangle.$$

This results in Eq.(8) in the main text.

2. Numerical check of the twining method

We shall numerically compare the results obtained by the twinning method with those obtained by the usual method of the wavepacket propagation in the action space of the linear subsystem, where the M -dimensional action space is spanned by the set truncated action basis with the Hilbert-space dimension N_i ($1 \leq i \leq M$).

Figure 5 shows the ΔJ^2 as a function of time for $M = 1$ and $M = 2$ with a given set of parameters. It can be seen that as the number of Hilbert-space dimension N_1 and N_2 of the action spaces increases, the results approaches to those obtained by the twin method, where the FFT-method is applied in the direct wavepacket propagation.

Figure 6 shows the ΔJ^2 as a function of time for various coupling strength η in the cases of $M = 1$ and $M = 2$ for large enough $N_1 = N_2$. It can be seen that the results from both methods agree well.

If diffusion like behavior takes place in the linear subsystem, the truncated dimension N_1, N_2, \dots, N_M must be increased in proportion to the diffusion length $\propto t^{1/2}$.

as the time-scale of simulation t increases. And the direct method requires the CPU time $\propto t^{1+M/2}$. On the other hand, the CPU time required for the twin method increases only as $\propto t$. Incidentally the CPU time required for the twin method is 70 seconds, while the direct method requires 36×10^3 seconds for $N_1 = N_2 = 256$ for the results of the Fig.5(b). These facts truly demonstrate the usefulness of the twin method. However, we also note that the twin method is applicable only for the case of linear subsystems. That is, we can call it poor man's method for poor man's model.

Appendix B: Localization length for $M = 1$ and $M = 2$

Some properties of localization length ℓ characterizing the dynamical localization observed for $M = 1$ and 2 are presented when the main system is hyperbolic Arnold cat map. Prior to showing the results, we briefly comment on the classical dynamics of the linear systems. Regarding Eq.(4) as the classical equation, the n -step local diffusion

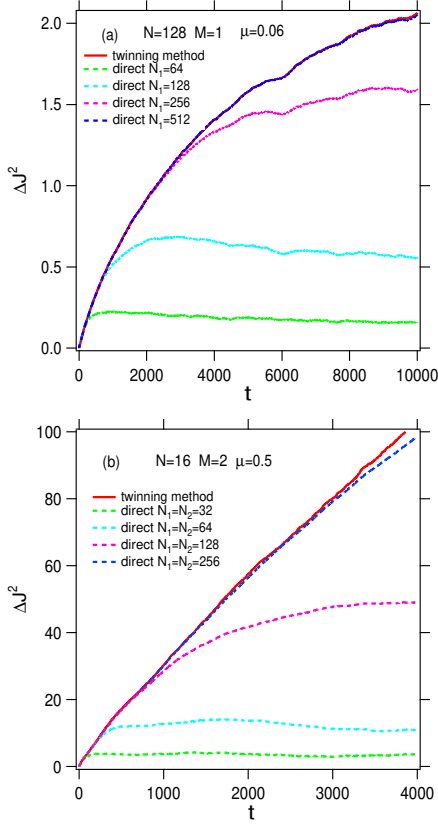


FIG. 5: (Color online) Comparison between the results using the twinning method and the direct method in the perturbed cat map of $K = -1$. (a) ΔJ^2 as a function of time for $\eta = 0.06$ and $N = 128$ in the monochromatically perturbed cat map ($M = 1$). $N_1 = 64, 128, 256, 512$. (b) ΔJ^2 as a function of time for $\eta = 0.5$ and $N = 16$ in the dichromatically perturbed cat map ($M = 2$). $N_1 = N_2 = 32, 64, 128, 256$.

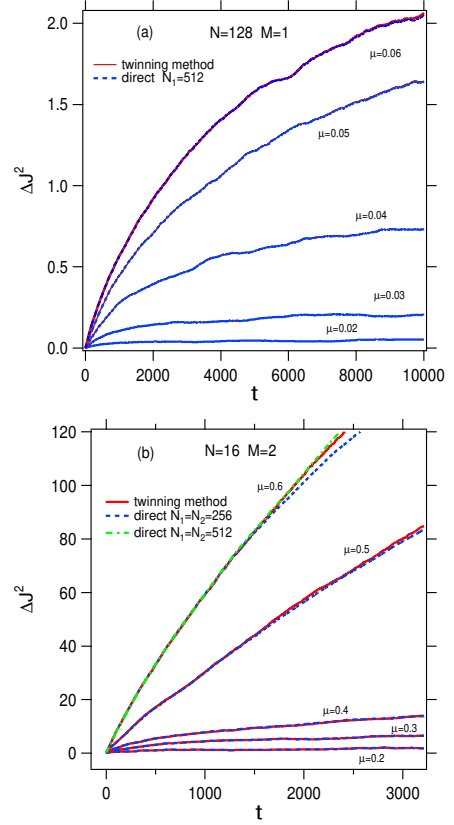


FIG. 6: (Color online) ΔJ^2 as a function of time for various η in (a) the monochromatically perturbed cat map ($M = 1$) of $K = -1$ and $N = 2^7$ and (b) in the dichromatically perturbed cat map ($M = 2$) of $K = -1$ and $N = 2^4$. The numerical results by using the twinning method and the direct method using FFT are shown by red solid line and blue dashed lines, respectively. Note that the all axes are in the linear scale.

constant $D_{cl}(n)$ can be defined by

$$D_{cl}(n) = \eta^2 [c(n, n) + 2 \sum_{n' < n} c(n, n')],$$

and

$$(J(t) - J(0))^2 = \sum_{n \leq [t]} D_{cl}(n)$$

where $c(n, n') = w'_k(\omega_k n) w'_k(\omega_k n') v(q_n) v(q_{n'})$ is correlation function. If the main system is fully chaotic and $\eta \ll 1$, the feature of chaos of the main system is not modified by the perturbation of linear modes, and for $t \rightarrow \infty$ the average $D_{cl} := \sum_{n=0}^{[t]} D_{cl}(n) / [t]$ converges to give the classical diffusion constant which obeys $\propto \eta^2$. In particular for the hyperbolic cat map the correlation function decays suddenly to give

$$D_{cl} = \eta^2 / 4$$

if $w_k(\phi) = \cos(\phi)$ and $v(q) = \cos(q)$. These facts can easily be confirmed by numerical simulation.

With this result we can conjecture that if the diffusion along a linear mode stops due to the quantum effect the localization length ℓ will be proportional to the scaled parameter $\eta^2 N^2$. Let us examine the case of $M = 1$. If the diffusion stops at n_s -step with the localization length ℓ , the classical results leads to $n_s D_{cl} = \ell^2$. The number of quantum state related to the suppressed diffusion is $N_{loc} = N \times [\text{number of action states in } \ell] = N\ell/\hbar$. Since the interval of quantum eigen angle is roughly $2\pi/N_{loc}$, the diffusion terminates at $n_s \sim N_{loc}$. These relations results into

$$\ell \propto N^2 \eta^2 \sim D_{cl} N^2 \quad \text{for } M = 1.$$

The numerical results shown in Figure 7(a) agrees quite with the predicted dependency on the combined parameter $\eta^2 N^2 \sim D_{cl} N^2$.

The above intuitive argument can not be extended to the case of $M = 2$. The numerical results reveals a quite different nature of ℓ which increases exponentially with D_{cl} and N . However, the combined parameter $\eta^2 N^2$ still plays a central role for $M = 2$. Figure 7(b) shows that

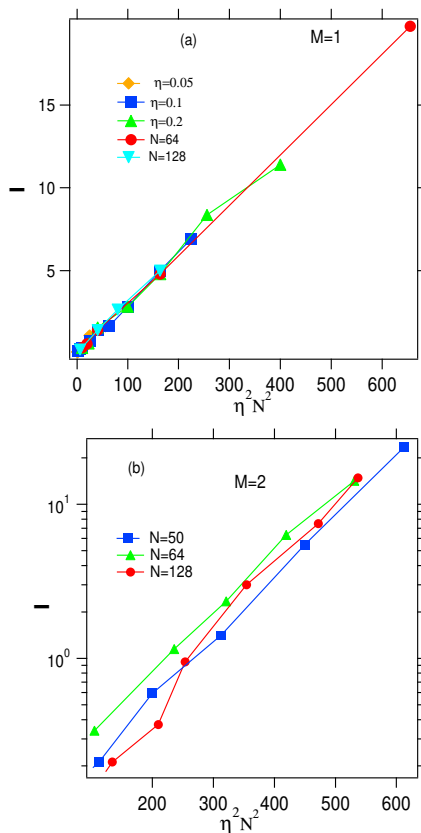


FIG. 7: (Color online) Dynamical localization length of the linear mode J_1 as a function of $\eta^2 N^2 (\propto \eta^2 D_{cl})$ for some parameters in the perturbed cases $M = 1$ (a) and $M = 2$ (b). Note that the vertical axis is in the linear scale for $M = 1$ and in the logarithmic scale for $M = 2$, respectively.

exponential growth of the localization length is also almost controlled by the combined parameter $N^2 D_{cl}$. As a result, the dynamical localization length can be summarized as follows:

$$\ell \propto e^{c_1 \eta^2 D_{cl}} \quad \text{for } M = 2,$$

where c_1 is a numerical constant. Similar phenomena have been observed in large quantum chaos system with infinite Hilbert-dimension such as perturbed standard map [28] and perturbed Anderson map [29].

Appendix C: Transition to diffusion in case of small N and $M = 3$

As shown in Fig.1(b) in the main text, a transition to diffusion takes place with increase of η even if the Hilbert space dimension N is not large. The nature of the transition is, however, different from the case of $N \gg 1$ in which a clear critical state with a definite critical index $\alpha_c < 1$ exists at a critical value $\eta = \eta_c$. Instead, there seems to be a transition range of η : if η is taken in the

transition range, the time-dependent index $\alpha(t)$ defined by Eq.(8) fluctuates notably as a function of time around a certain value $\bar{\alpha}$ as is depicted in Fig.8 and the mean value $\bar{\alpha}$ tends to increase with η and approaches the line $\alpha = 1$ beyond 0.4. For the different choice of initial state, the pattern of the fluctuation is quite similar as shown in Fig.8. It means that the insensitivity of the fluctuation to the initial state and has a quantum origin.

The occurrence of stationary diffusion implies the correlation function $c(n, n')$ in the last section converges and loss of memory is maintained. The mechanism by which such an apparently irreversible behavior is self-organized in integrable systems by coupling with very small quantum chaos consisting of only a few quantum states is an important issue. We have currently no theoretical tools to attack the issue.

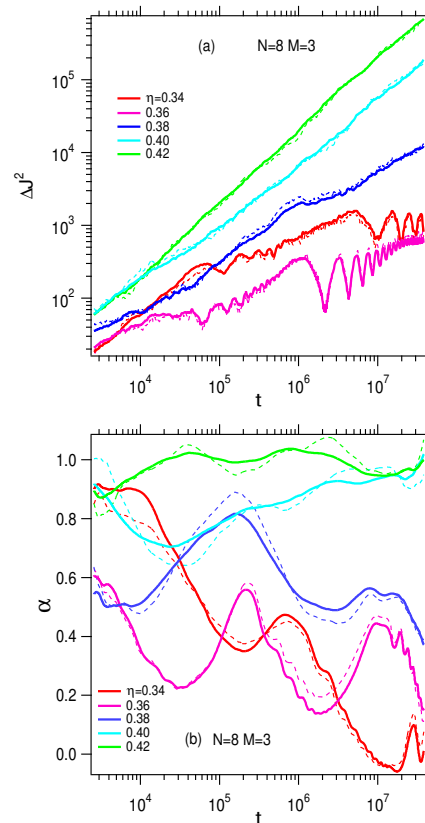


FIG. 8: (Color online) (a) ΔJ^2 as a function of time for various η in the trichromatically perturbed cat map ($M = 3$) of $K = -1$ and $N = 2^3$. (b) Plots of α as a function of t for various η . The results for a single initial state $|\phi_0\rangle$ (by broken lines) and the average over 8 orthogonal random $|\phi_0\rangle$ (by thick solid lines) are compared. The patterns of fluctuation almost coincide.

Acknowledgments

This work is supported by Japanese people's tax via MEXT/JSPS KAKENHI Grant Number 22K03476 and

22H01146, and the authors would like to acknowledge them. The authors are also thankful to Kankikai (Dr. T. Tsuji) and Koike memorial house for using the facilities during this study.

-
- [1] A.J. Lichtenberg and M.A. Lieberman, *Regular and Chaotic Dynamics* (Applied Mathematical Sciences 38), (Springer; 2nd ed. 1992).
- [2] B.V.Chirikov, Phys. Rep. **52** 263 (1979).
- [3] V.I. Arnol'd, Soviet Mathematics-Doklady **5**, 581-5(1964).
- [4] N. N. Nekhoroshev, Usp. Mat. Nauk **32**, 5 (1977).
- [5] M. A. Lieberman, Ann. N. Y. Acad. Sci. **357**, 119 (1980).
- [6] P. J. Holmes and J. E. Marsden, J. Math. Phys. **23**, 669(1982).
- [7] K. Kaneko and Richard J. Bagley, Phys.Lett. A **110** 435-440(1985).
- [8] P.M.Cincotta *et al.*, Physica D **266**, 49-64(2014).
- [9] M.S. Santhanam, S. Paul, and J. BharathiKannan, Physics Reports **956**, 1-87(2022).
- [10] S. S. Maurya, J. B. Kannan, K. Patel, P. Dutta, K. Biswas, J. Mangaonkar, M. S. Santhanam, and U.D. Rapol, Phys. Rev. E **106**, 034207(2022).
- [11] Y.Boretz, and L. E. Reichl. Phys. Rev. E **93**,032214(2016).
- [12] David M. Leitner and Peter G. Wolynes, Phys.Rev. Lett. **79**, 55-58(1997).
- [13] V.Ya. Demikhovskii, F.M. Izrailev, and A.I. Malyshev, Phys.Rev. Lett. **88**, 154101(2002).
- [14] V.Ya. Demikhovskii, F.M. Izrailev, and A.I. Malyshev, Phys. Rev. E **66**, 036211(2002).
- [15] V.Ya. Demikhovskii, F.M. Izrailev, and A.I. Malyshev, Phys. Lett. A **352**, 491 (2006).
- [16] G. Casati, B. V. Chirikov, F. M. Izrailev, J.Ford, *Stochastic behavior of a quantum pendulum under a periodic perturbation* (Springer-Verlag,Berlin,1979) ed. by G.Casati and J.Ford, pp334.
- [17] S. Fishman, D.R.Grempel, R.E.Prange, Phys. Rev. Lett. **49**, 509 (1982).
- [18] G.Casati, I.Guarneri and D.L.Shepelyansky, Phys. Rev.Lett. **62**, 345(1989).
- [19] L. Chotorlishvili, S. Stagracynski, M. Schlerc and J. Berakdar, ACTA PHYSICA POLONICA A **135** 1155-1161(2019).
- [20] S. Adachi, M. Toda, and K. Ikeda, Phys. Rev. Lett. **61**, 659(1988).
- [21] B.Gadway, J.Reeves, L.Krinner, D.Schneble Phys. Rev. Lett. **110**, 190401(2013).
- [22] M.Lopez, J.F.Clement, P.Szrftgiser, J.C.Garrau, and D.Delande, Phys. Rev. Lett. **108**, 095701(2012).
- [23] M. Lopez, J.-F. Clement, G. Lemarie, D. Delande, P. Szrftgiser, and J. C. Garreau, New J. Phys. **15**, 065013(2013).
- [24] H.S.Yamada and K.S.Ikeda Phys. Rev. **E101**, 032210 (2020).
- [25] D.L. Shepelyansky, Physica D **8**,208-222(1983).
- [26] J.Chabe,G.Lemarie,B.Gremaud, and D.Delande, P.Szrftgiser, and J.C.Garrau, Phys. Rev. Lett. **101**, 255702(2008).
- [27] G.Lemarie, J.Chabe, P.Szrftgiser, J.C.Garrau, B.Gremaud, and D.Delande, Phys. Rev. A **80**, 043626(2015).
- [28] I.Manai, J.F.Clement, R.Chicireanu, C.Hainaut, J.C.Garrau, P.Szrftgiser, and D.Delande, Phys. Rev. Lett. **115**, 240603(2015).
- [29] H.S.Yamada F.Matsui, and K.S.Ikeda, Phys. Rev. **E 97**, 012210 (2018).